On the role of groundwater and soil texture in the regional water balance: An investigation of the Nebraska Sand Hills, USA

Tiejun Wang,[1] Erkan Istanbulluoglu,[2] John Lenters,[1,3] and Durelle Scott[4]

Received 13 January 2009; revised 26 May 2009; accepted 4 August 2009; published 9 October 2009.

[1] Partitioning of precipitation between evapotranspiration and runoff at the basin scale is primarily controlled by climate and basin characteristics. Here we use the Budyko hypothesis to investigate the impacts of soil texture and groundwater (e.g., baseflow) on annual and long-term mean annual water balances of basins in a semiarid region located in and around the Sand Hills region of Nebraska, USA. Native grasslands are dominant across the study area with soil textures dramatically different for the Nebraska Sand Hills (primarily sand deposits) and the adjacent regions (mainly less permeable silt loam). For each basin, long-term hydrologic and meteorological data are obtained, and a baseflow index is calculated using daily streamflow data to quantify the groundwater contribution to streamflow. We found sound field evidence that suggests the control of soil texture on mean annual water balance and the impact of groundwater storage on interannual variability of water balance at catchment scales, which is usually seen at plot scales and in theoretical models. Our results show that compared to the basins located in the adjacent regions, the Nebraska Sand Hills basins experience much higher long-term mean annual surface runoff ratios ($\overline{R}/\overline{P}$) and thus lower ratios of $(\overline{P}-\overline{R})/\overline{P}$, where $\overline{P}$ is the long-term mean annual precipitation. The high baseflow index and its positive correlation with the ratio of $\overline{R}/\overline{P}$ in the Sand Hills basins illustrate the role of lower (higher) evapotranspiration (recharge) rates. On annual time scales, the baseflow-dominated basins exhibit a negative relationship between annual $(P-R)/P$ and annual aridity index (i.e., the ratio of annual potential evapotranspiration to annual precipitation), which deviates from the original Budyko hypothesis. Moreover, with decreasing baseflow index, this negative relationship gradually transits into a positive relationship that follows Budyko's curves. Our results suggest that soil textural differences may strongly modify the impact of climate on regional water balance. These findings may have important implications for managing water resources under a fluctuating climate.

Citation: Wang, T., E. Istanbulluoglu, J. Lenters, and D. Scott (2009), On the role of groundwater and soil texture in the regional water balance: An investigation of the Nebraska Sand Hills, USA, *Water Resour. Res.*, *45*, W10413, doi:10.1029/2009WR007733.

1. Introduction

[2] Evaluation of basin water balance is among the fundamental tasks in hydrology for predicting runoff in ungauged basins, assessing hydrologic implications of anthropogenic disturbances and climate change, identifying dominant hydrologic processes of basins, and constructing and applying regional hydrology models [*Zhang et al.*, 2001, 2004, 2008; *Wagener et al.*, 2007]. The hydrologic response of a basin to external forcings (e.g., climate and anthropogenic activities) is a reflection of complex interactions between biotic and abiotic processes within it. Despite these complexities, a number of studies have shown that basin hydrology over long time scales may be explained by simple conceptual models for the partitioning of precipitation into evapotranspiration and runoff [*Wagener et al.*, 2007]. By synthesizing earlier studies and analyzing runoff and precipitation data from basins in a wide range of climates, *Budyko* [1958, 1974] postulated that the mean annual actual evapotranspiration ($\overline{ET_a}$) of a basin asymptotically approaches the mean annual precipitation ($\overline{P}$) as the climate gets drier. The climatic dryness can be represented by an aridity index, $\overline{\Phi} = \overline{ET_p}/\overline{P}$, where $\overline{ET_p}$ is the maximum or potential mean annual evapotranspiration. Assuming that precipitation is in balance with runoff and actual evapotranspiration on a mean annual basis, and interbasin groundwater flow is negligible, basin water balance normalized with respect to precipitation can be written as:

$$\frac{\overline{R}}{\overline{P}} + \frac{\overline{ET_a}}{\overline{P}} = 1 \tag{1}$$

[1] School of Natural Resources, University of Nebraska, Lincoln, Nebraska, USA.
[2] Department of Civil and Environmental Engineering, University of Washington, Seattle, Washington, USA.
[3] Department of Geosciences, University of Nebraska, Lincoln, Nebraska, USA.
[4] Department of Biological Systems Engineering, Virginia Polytechnic Institute and State University, Blacksburg, Virginia, USA.

0043-1397/09/2009WR007733

The Budyko hypothesis suggests that,

$$\frac{\overline{ET_a}}{\overline{P}} = \begin{cases} F(\overline{\Phi}) \to 0, & \overline{\Phi} \to 0 \\ & \text{and} \\ F(\overline{\Phi}) \to 1, & \overline{\Phi} \to \infty \end{cases}$$
$$\frac{\overline{R}}{\overline{P}} = \begin{cases} \left[1 - F(\overline{\Phi})\right] \to 1, & \overline{\Phi} \to 0 \\ \\ \left[1 - F(\overline{\Phi})\right] \to 0, & \overline{\Phi} \to \infty \end{cases} \quad (2)$$

where $\overline{R}$ is basin runoff at a defined outlet that combines both surface, subsurface, and groundwater flow contributions, and $F(\overline{\Phi})$ is an empirical function that estimates the fraction of evapotranspiration in precipitation. The Budyko hypothesis has been widely used as a conceptual framework for examining basin water balance in a range of climates and environmental conditions, and for developing and validating regional hydrologic models [*Milly*, 1994; *Choudhury*, 1999; *Koster and Suarez*, 1999; *Zhang et al.*, 2001, 2004, 2008; *Atkinson et al.*, 2002; *Farmer et al.*, 2003; *Porporato et al.*, 2004]. Those studies have underscored that in addition to the aridity index, factors such as climate seasonality, soil water-holding capacity, and vegetation also control the partitioning of precipitation into evapotranspiration and runoff. Using a stochastic model, *Milly* [1994] proposed seven dimensionless ratios to characterize basin hydrology, which included soil properties (e.g., soil water-holding capacity) and climate seasonality. By compiling data from over 250 basins globally, *Zhang et al.* [2001] incorporated the role of vegetation in $F(\overline{\Phi})$. Some recent efforts have also used the Budyko hypothesis for hydrologic prediction over annual [*Koster and Suarez*, 1999; *Arora*, 2002; *Zhang et al.*, 2008] and monthly [*Zhang et al.*, 2008] scales with reasonable success. However, as evident in equation (1), the Budyko hypothesis implicitly assumes steady-state conditions with no change in basin water storage, which might limit predictions over time scales shorter than the residence time of basin water storage.

[3] The roles of different sources of streamflow (e.g., surface, subsurface, and groundwater) as well as the impact of soil texture have not been adequately addressed within Budyko's framework, while these factors have been examined in other numerical modeling approaches [*Milly*, 1994; *Rodriguez-Iturbe and Porporato*, 2004; *Small*, 2005]. Because Budyko's curve reflects the combined effect of surface and subsurface processes on basin evapotranspiration and runoff, soil texture is expected to have a control on its shape. As a corollary to this, the time scales, over which basins attain a hydrologic steady-state, depend on many factors including soil, vegetation, climate, and dominant sources of runoff. For example, in baseflow-dominated basins, conceptualizing evapotranspiration as a closure term in water balance equations may require much longer time series data on runoff and precipitation, as groundwater travels much slower than surface and subsurface flows. Moreover, groundwater storage-release behavior mostly relies on hydrologic boundary conditions and groundwater recharge [*Brutsaert and Nieber*, 1977; *Brutsaert*, 2008], soil properties [*De Vries and Simmers*, 2002; *Small*, 2005], and basin morphology [e.g., *Marani et al.*, 2001].

[4] In this paper, we focus on the following two interrelated research questions: (1) What are the roles of soil texture and groundwater (e.g., baseflow) in controlling mean annual and interannual basin water balance? and (2) How can surface water- and groundwater-driven systems that behave differently with respect to basin runoff generation be distinguished and evaluated using the Budyko hypothesis? Here we use the Budyko hypothesis as a framework to diagnose and examine basin water balance in relation to soil texture and baseflow contribution. These questions are addressed using basins within and around the Nebraska Sand Hills, the largest native grassland-stabilized sand dune field in the Western Hemisphere [*Loope and Swinehart*, 2000, Figure 1]. Due to the high infiltration capacity of sandy soils, the Sand Hills is a major recharge area for the Ogallala aquifer underlying the Great Plains of the United States [*Bleed and Flowerday*, 1989; *Wang et al.*, 2008, 2009b]. High levels of regional groundwater tables lead to a dominant baseflow control in the Sand Hills streams [*Chen et al.*, 2003]. As such, the region presents a natural field experiment to study the hydrologic response of catchments to climate variability with varying degrees of groundwater contribution. Furthermore, despite both the hydrologic and ecological importance of the Sand Hills [*Loope and Swinehart*, 2000], studies on basin water balance in this region are very limited and have mainly focused on the perspective of groundwater recharge [*Szilagyi et al.*, 2003, 2005].

[5] In what follows, we first describe the climate, soils, and ecology in the study area as well as the hydrologic data used in this study, followed by our methods for analyzing the mean annual and interannual water balance of basins in the study area. By synthesizing baseflow, runoff, and precipitation, as well as observed and predicted trends in the relationship between $(P - R)/P$ and Φ, we discuss how the Budyko hypothesis may be used to diagnose the dominant hydrologic processes of a basin for determining basin runoff generation and the hydrologic response of a basin to climate changes.

2. Study Area

[6] Three major rivers that flow in the west-east direction across central Nebraska (drainage areas given in parentheses), including the Elkhorn (18,100 km^2), the Loup (39,200 km^2), and the Niobrara (39,900 km^2), are examined in this study (Figure 1). The selected rivers are perennial with year-round flows. As permitted by the availability of streamflow data, a total of 34 subbasins within these river basins are selected with drainage areas ranging from 750 km^2 to 18,500 km^2 (Table 1). The Nebraska Sand Hills covers approximately 50.3% of the entire area studied (Figure 1). The 58,000-km^2 Nebraska Sand Hills is the largest native grassland-stabilized sand dune area in the Western Hemisphere [*Loope and Swinehart*, 2000]. The region is mostly covered by Holocene eolian sand deposits overlying Quaternary and/or Pliocene alluvial sand and silt; whereas, the adjacent regions mainly consist of less permeable soils, mostly silt loam [*Bleed and Flowerday*, 1989; *Wang et al.*, 2008, 2009b; STATSGO, http://www.dnr.state.ne.us/databank/soilsall.html]. The regional climate is semiarid with a significant precipitation gradient from about 450 mm/a in the west to over 650 mm/a in the east [*Szilagyi et al.*, 2003]. Climate seasonality was shown to affect the shape of the Budyko curve [*Porporato et al.*, 2004; *Yokoo et al.*, 2008].

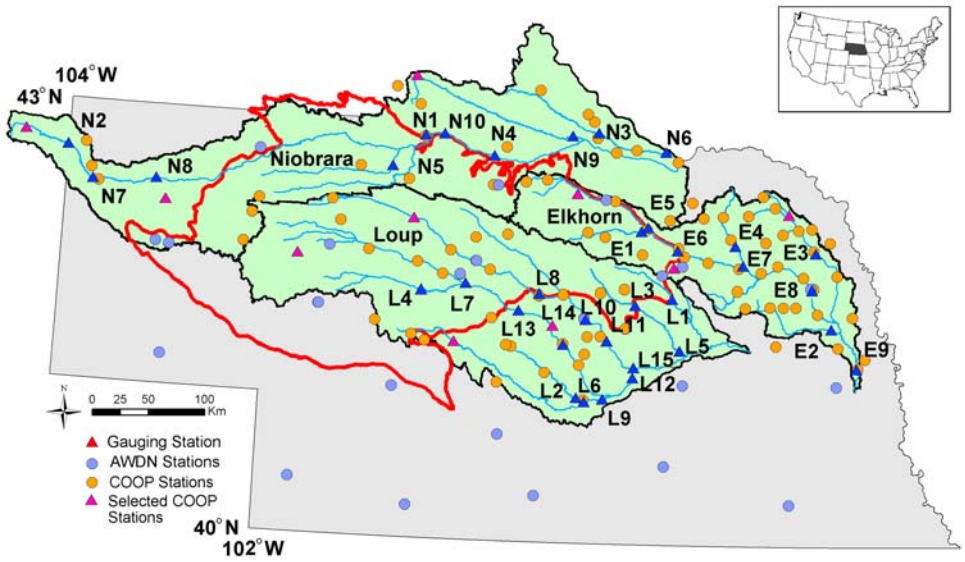

Figure 1. Location map of the Nebraska Sand Hills (thick, red line) and three major river systems in the study area with their drainage basins: Loup River Basin, Elkhorn River Basin, and Niobrara River Basin. Pink triangles are the COOP meteorological stations used for the representation of climate seasonality in the study area (Figure 2).

Mean daily precipitation and temperature from 10 weather stations across the region are shown in Figure 2. In general, the area can be characterized by continental climate with most precipitation falling in summer seasons (Figure 2). Native warm (C_4) grasslands are dominant in this region with limited croplands mainly composed of alfalfa and corn [*Dappen et al.*, 2007]. The high infiltration capacity of sandy soils makes the Sand Hills an important groundwater recharge area for the Ogallala aquifer [*Bleed and Flowerday*, 1989; *Wang et al.*, 2008, 2009b]. The regional groundwater flow follows the topography in the region with higher groundwater tables in the Sand Hills compared to the adjacent areas [*Bleed and Flowerday*, 1989]. The resulting aquifer thickness exhibits a strong spatial gradient decreasing from the western and central Sand Hills towards its boundaries [*McGuire and Fischer*, 1999], leading to a stronger

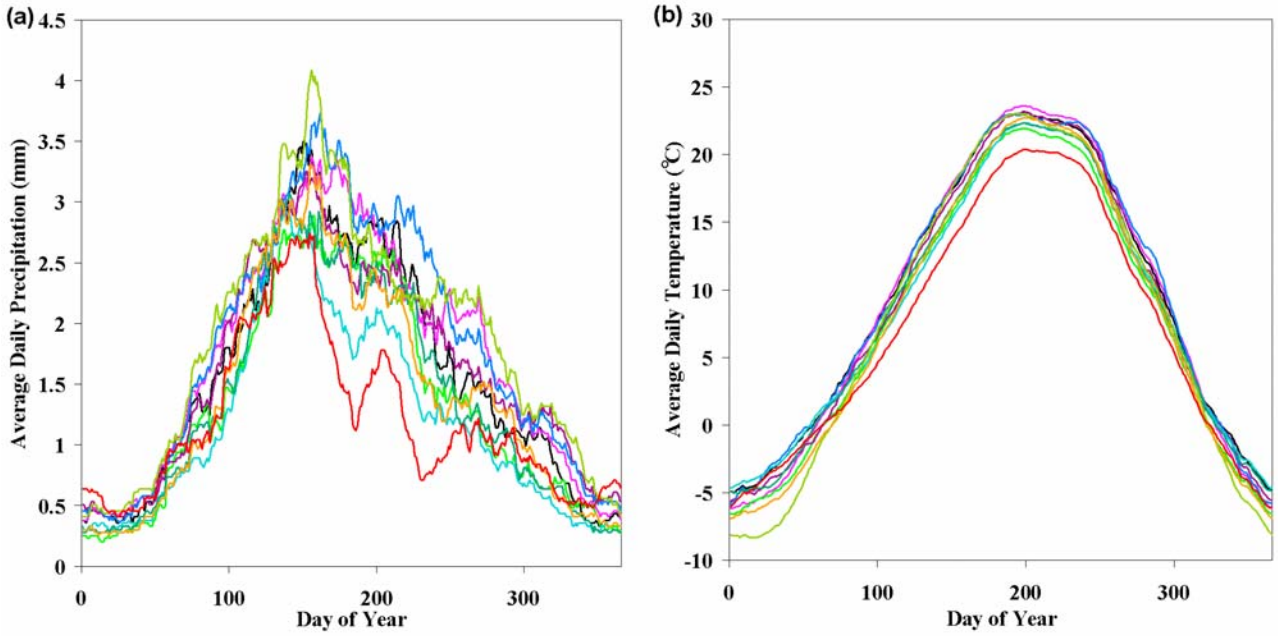

Figure 2. Average daily precipitation and temperature plotted with respect to day of the year from 10 COOP meteorological stations uniformly located across the study area (see Figure 1 for locations), depicting the climate seasonality of the study area.

Table 1. Summary of Gauging Stations, Drainage Area, Length of Annual Records, Percent of Drainage Area in the Nebraska Sand Hills, and Primary Soil Texture of Each Sub-basin

Subbasin ID	Gauging Station for Defining the Subbasin	USGS ID	Drainage Area (km^2)	Length of Annual Records (years)	Percentage of Drainage Area in the Sand Hills (%)	Primary Soil Texture
E1	South Folk Elkhorn River at Ewing	06798000	754.6	29	100	loamy sand and sand
E2	Maple Creek near Nickerson	06800000	954.9	55	0	silt loam
E3	Logan Creek at Pender	06799450	1906.6	27	0	silt loam
E4	North Fork Elkhorn River near Pierce	06799100	2013.7	46	0	silt loam
E5	Elkhorn River at Ewing	06797500	3686.4	59	92	loamy sand and sand
E6	Elkhorn River at Neligh	06798500	5923.1	59	91	loamy sand and sand
E7	Elkhorn River at Norfolk	06799000	7416.4	61	74	silt loam and loamy sand
E8	Elkhorn River at West Point	06799350	12111.9	34	45	silt loam and loamy sand
E9	Elkhorn River at Waterloo	06800500	18094.6	76	30	silt loam
L1	Beaver creek at Loretto	06793500	987.5	19	90	sand
L2	Mud Creek at Sweetwater	06783500	1839.2	47	0	silt loam
L3	Cedar River at Spalding	06791500	1945.3	44	98	sand
L4	Dismal River at Thedford	06775900	2503.1	40	100	sand
L5	Cedar River at Fullerton	06792000	3147.7	54	64	sand and silt loam
L6	South Loup at Ravenna	06782500	3918.8	24	26	silt loam
L7	Middle Loup River at Dunning	06775500	4492.3	61	100	sand
L8	North Loup River at Taylor	06786000	6085.8	70	99	sand
L9	South Loup River at Saint Michael	06784000	6243.6	63	16	silt loam
L10	North Loup River at Ord	06788500	9759.0	41	90	sand
L11	North Loup River at Scotia	06789000	10282.8	33	86	sand
L12	North Loup River at Saint Paul	06790500	11210.8	76	79	sand
L13	Middle Loup at Walworth	06777500	11784.6	19	96	sand
L14	Middle Loup River at Arcadia	06779000	12814.0	32	88	sand
L15	Middle Loup River at Saint Paul	06785000	14543.1	44	78	sand and silt loam
N1	Minnechaduze Creek at Valentine	06461000	1000.3	46	49	sand and sandy loam
N2	Niobrara River at Wyo-Neb State Line	06454000	1180.8	38	0	silt loam
N3	Ponca Creek at Anoka	06453500	1303.5	44	0	silt loam
N4	Plum Creek at Meadville	06462500	1391.0	44	94	sand
N5	Snake River at Burge	06459500	1646.9	31	100	sand
N6	Ponca Creek at Verdel	06453600	2102.1	49	0	silt loam
N7	Niobrara River at Agate	06454100	2426.0	33	0	silt loam and loamy sand
N8	Niobrara River above Box Butte Reservoir	06454500	3693.9	47	0	silt loam and loamy sand
N9	Keya Paha River at Naper	06464900	4377.8	36	0	silt loam
N10	Niobrara River at Sparks	06461500	18518.4	61	65	sand and loamy sand

groundwater influence on streamflow in the Sand Hills rivers than those outside of the Sand Hills [*Chen et al.*, 2003].

3. Methods

3.1. Budyko's Framework and Methodology

[7] We use the Budyko hypothesis as a conceptual model to evaluate and diagnose the interannual and long-term mean annual water balance of basins with varying soil textures. The Budyko hypothesis [*Budyko*, 1974] postulates that $\overline{ET_a}/\overline{P}$ is positively correlated with $\overline{\Phi}$, when the long-term change in basin water storage is negligible. Analytical equations have been proposed to delineate Budyko's curve, which often use $\overline{\Phi}$ as the only input [*Arora*, 2002]. In this study, we use the function proposed by *Zhang et al.* [2001]:

$$\frac{\overline{ET_a}}{\overline{P}} \approx \frac{\overline{P}-\overline{R}}{\overline{P}} = F\left(\overline{\Phi}, w\right) = \frac{1+w\overline{\Phi}}{1+w\overline{\Phi}+\overline{\Phi}^{-1}} \qquad (3)$$

where w is termed the "plant-available water coefficient." By fitting equation (3) into a dataset containing over 250 basins globally, *Zhang et al.* [2001] found that the optimal value of w is 2.0 for forested basins and 0.5 for grassed basins. The difference in w values is largely due to higher evapotranspiration rates of forests under similar climatic conditions [*Zhang et al.*, 2001]. Later, *Zhang et al.* [2004] suggested the use of w as a lumped factor to represent the integrated effect of multiple basin processes and land cover conditions on evapotranspiration. In the application of the Budyko hypothesis, the change in basin water storage (ΔS) is often assumed to be negligible over long-term mean annual time scales (albeit without any clear definition of the minimum time scales necessary for $\Delta S \approx 0$), and actual basin evapotranspiration is approximated based on the water balance equation, such that $\overline{ET_a} \approx \overline{P} - \overline{R}$. If ΔS is negligible, the $(\overline{P}-\overline{R})/\overline{P}$ vs. $\overline{\Phi}$ data pairs from basins in a range of climates often follow an asymptotic relation (e.g., equation (3)). In this paper, we use equation (3) to compare the predicted and observed trends in the $(P-R)/P$ vs. Φ relationship on both interannual and long-term mean annual time scales for selected subbasins with varying Sand Hills coverage and baseflow contributions in the study area. Soil, hydrology, and climate data compiled for these purposes are described below.

3.2. Soil Type

[8] The primary soil texture of the topsoil in each subbasin obtained from the STATSGO database is reported in Table 1. The fraction of basin drainage area contained within the Sand Hills is calculated for each subbasin. Because sandy soils are prevalent in the Sand Hills, this ratio thus reflects the approximate percentage of the drainage area covered by sand for each subbasin. Despite soil

textures in the Sand Hills are relatively uniform, soil hydraulic characteristics are expected to show some spatial variability within the Sand Hills. For example, in a Sand Hills study, *Wang et al.* [2008, 2009b] reported saturated hydraulic conductivities of vadose zone varying between 200 and 1500 cm/day at plot scales of about 100 m, and related this variability to subtle differences in particle size distribution, soil depth, topographic position, and root density.

3.3. Hydrologic Data and Analysis

[9] Streamflow data for each subbasin (varying between 19 and 76 years of record) are obtained from the National Water Information System operated by the United States Geological Survey (USGS; http://waterdata.usgs.gov/nwis). Basin IDs, drainage areas, USGS gauge station IDs, and the periods of streamflow records are reported in Table 1. Annual precipitation for each subbasin is obtained from the Parameter-elevation Regressions on Independent Slopes Model (PRISM) data set, a widely used spatial database on precipitation and temperature across the continental United States [http://www.ocs.oregonstate.edu/prism/; *Daly et al.* 1994, 2002]. The PRISM system uses over 8000 point measurements of precipitation, temperature, and other climatic data to estimate monthly and yearly precipitation with a 4-km $\times$ 4-km spatial resolution. In each subbasin, spatially distributed annual precipitation is obtained from the PRISM data set and then averaged to estimate basin-scale annual precipitation (P [mm/a]). Long-term mean annual precipitation ($\overline{P}$ [mm/a]) is obtained by averaging basin-scale annual precipitation over the duration with available streamflow data. Annual basin runoff R [mm/a] is calculated by dividing the total volume of annual streamflow by the drainage area of each basin, and long-term mean annual runoff ($\overline{R}$ [mm/a]) is obtained by averaging basin annual runoff over the period of data. We make the assumption that runoff is mainly driven by precipitation falling within the topographic boundary of each basin. In the study area, regional groundwater maps show that the groundwater table divides follow the topographic boundary of each subbasin and that elevations of groundwater tables in the Sand Hills are generally higher compared to the adjacent regions (see reports on Annual Evaluation of Availability of Hydrologically Connected Water Supplies, Nebraska Dept. of Natural Resources, http://www.nlc.state.ne.us/epubs/N1500/A005.html). For the sake of clarity, we present the water-balance estimates of actual evapotranspiration in each subbasin by ($P - R$) and ($\overline{P} - \overline{R}$) instead of ET_a and $\overline{ET_a}$ (see equation (3)), as precipitation and runoff are directly measured, whereas basin-wide observations or independent estimates of ET_a are not available for this region. It is, of course, generally assumed that $ET_a = P - R$ for sufficiently long timescales, but we do not wish to constrain ourselves to this assumption. As such, this notation is also adopted to avoid any reader confusion.

[10] To calculate the annual and long-term mean annual aridity index needed for equation (3), an estimate of potential evapotranspiration is necessary. The types of meteorological variables measured in the region vary by location and time period. To take full advantage of the streamflow data, we used net radiation and air temperature-based Priestley-Taylor [*Priestley and Taylor*, 1972] and only air temperature-based Hargreaves [*Hargreaves and Samani*, 1982] equations.

[11] The Priestley-Taylor equation, employed in earlier studies for investigating the Budyko hypothesis [*Zhang et al.*, 2001, 2004] and grassland ecohydrology [*Williams and Albertson*, 2005], can be written as:

$$ET_p = 1.26\frac{\Delta}{\Delta+\gamma}R_n \tag{4}$$

where Δ is the slope of the saturation vapor pressure curve calculated as a function of air temperature, γ is the psychometric constant, and R_n is the water equivalent of net radiation (mm/day). Inputs to equation (4) are obtained from the Automated Weather Data Network stations (AWDN; Figure 1) operated by the High Plains Regional Climate Center at the University of Nebraska. The length of daily weather data for AWDN stations varies, but often limited to about 25 years. To calculate basin-scale annual ET_p, the AWDN stations with averaged 21-year records in the Elkhorn, Loup, and Niobrara river basins as well as those within a 30-km basin radius are selected. Annual ET_p at each AWDN station is calculated as the summation of daily ET_p. Because the distribution of the selected AWDN stations is considerably uniform over a relatively flat topography, the spatially averaged annual ET_p for the basins are calculated as the arithmetic mean of annual station ET_p within each basin.

[12] The aridity index is a function of both annual ET_p and P. Typically in this region, precipitation and streamflow records cover much longer periods than the records of net radiation from AWDN stations. This requires adapting other methods for long-term calculations of aridity index when relevant climatic data are absent. For this, we developed empirical power functions of annual Φ versus P, as there seems to be a linkage between precipitation and net radiation through land surface processes [*Milly and Dunne*, 2002]. These relations are developed for the three major river basins using basin-scale P estimated from the PRISM data set and ET_p estimated by equation (3) as described above.

$$\text{Loup River Basin}: \Phi = 4194.0 \times P^{-1.1431}\left(r^2 = 0.90\right) \tag{5a}$$

$$\text{Elkhorn River Basin}: \Phi = 5295.5 \times P^{-1.1809}\left(r^2 = 0.94\right) \tag{5b}$$

$$\text{Niobrara River Basin}: \Phi = 4050.3 \times P^{-1.1414}\left(r^2 = 0.96\right) \tag{5c}$$

These functions are then used to calculate Φ for all time periods in the subsequent data analysis. We compared our empirically calculated aridity indices and potential evapotranspirations with those mapped by *Szilagyi et al.* [2003, 2005] at some selected locations, and found that the results well concur with each other.

[13] As an alternative to the empirical method described above, the temperature-based Hargreaves equation [*Hargreaves and Samani*, 1982] is used when air temperature is the only weather data other than precipitation reported

Table 2. Summary of Long-term Mean Annual Precipitation ($\overline{P}$), Runoff ($\overline{R}$), $\overline{R}/\overline{P}$, $(\overline{P}-\overline{R})/\overline{P}$, Aridity Index ($\overline{\Phi}$), and Baseflow Index (BFI) of Each Sub-basin

Subbasin ID	$\overline{P}$ (mm/a)	$\overline{R}$ (mm/a)	$\overline{R}/\overline{P}$	$(\overline{P}-\overline{R})/\overline{P}$	$\overline{\Phi}_1$[a]	$\overline{\Phi}_2$[b]	$\overline{\Phi}_3$[c]	BFI
E1	593.01	81.81	0.14	0.86	2.68	2.81	1.84	0.81
E2	709.28	72.91	0.10	0.90	2.21	2.28	1.54	0.59
E3	673.63	73.46	0.11	0.89	2.27	2.42	1.60	0.69
E4	661.48	45.89	0.07	0.93	2.36	2.47	1.64	0.74
E5	588.96	46.72	0.08	0.92	2.63	2.84	1.85	0.76
E6	565.23	45.65	0.08	0.92	2.66	2.98	1.96	0.80
E7	609.77	64.57	0.11	0.89	2.55	2.72	1.79	0.82
E8	647.64	73.08	0.11	0.89	2.45	2.54	1.67	0.80
E9	639.25	66.25	0.10	0.90	2.35	2.57	1.72	0.78
L1	639.80	73.38	0.11	0.89	2.68	2.61	1.73	0.80
L2	595.09	18.68	0.03	0.97	2.71	2.84	1.92	0.70
L3	601.63	76.31	0.13	0.87	2.63	2.80	1.86	0.92
L4	465.50	73.47	0.16	0.84	3.64	3.75	2.42	0.98
L5	608.78	72.78	0.12	0.88	2.56	2.76	1.83	0.86
L6	545.44	43.60	0.08	0.92	–	3.13	2.13	0.81
L7	501.21	84.78	0.17	0.83	3.37	3.45	2.26	0.97
L8	533.13	71.21	0.13	0.87	3.10	3.21	2.14	0.92
L9	576.99	33.14	0.06	0.94	2.91	2.94	1.98	0.83
L10	549.21	81.66	0.15	0.85	2.98	3.11	2.06	0.92
L11	528.42	75.19	0.14	0.86	–	3.25	2.17	0.90
L12	543.06	75.18	0.14	0.86	2.95	3.15	2.10	0.89
L13	509.80	60.59	0.12	0.88	–	3.38	2.25	0.94
L14	525.18	50.21	0.10	0.90	3.24	3.27	2.16	0.87
L15	530.72	69.62	0.13	0.87	3.17	3.23	2.10	0.85
N1	480.76	30.48	0.06	0.94	3.26	3.52	2.26	0.86
N2	395.37	2.75	0.01	0.99	4.12	4.40	2.75	0.87
N3	599.12	31.03	0.05	0.95	2.58	2.74	1.86	0.60
N4	549.90	76.17	0.14	0.86	2.94	3.02	2.31	0.93
N5	485.51	85.13	0.18	0.82	3.31	3.48	1.84	0.88
N6	602.19	36.94	0.06	0.94	2.67	2.72	2.94	0.67
N7	381.45	5.00	0.01	0.99	4.42	4.58	2.82	0.91
N8	394.84	6.96	0.02	0.98	4.22	4.40	2.09	0.89
N9	530.60	28.18	0.05	0.95	3.00	3.14	2.50	0.78
N10	442.73	36.99	0.08	0.92	3.69	3.87	1.84	0.94

[a]Mean annual aridity index based on Priestley-Taylor equation-based ET_p.
[b]Mean annual aridity index based on the empirically derived power functions (equation (5)).
[c]Mean annual aridity index obtained from the Hargreaves daily evapotranspiration model.

from a weather station. This model has been used earlier for estimating basin-wide ET_p and studying the Budyko hypothesis [*Sankarasubramanian et al.*, 2001; *Sankarasubramanian and Vogel*, 2002; *Vogel and Sankarasubramanian*, 2005] and can be written as:

$$ET_p = 0.0023 \times (T_{mean} + 17.8) \times (T_{\max} - T_{\min})^{0.5} \times Ra \quad (6)$$

where ET_p is daily potential evapotranspiration, T_{mean} is daily mean temperature, $T_{\max}$ and $T_{\min}$ are maximum and minimum daily temperature, respectively, and Ra is extraterrestrial radiation based on latitude of the location and month of the year [*Hargreaves and Samani*, 1982]. The required daily temperature data are obtained from the National Weather Service Cooperative network (COOP; Figure 1) with the earliest records starting from 1880s. For each subbasin, the COOP stations that are located both inside and within 10-km proximity of the subbasins are used. Annual ET_p at each COOP station is calculated as the summation of daily ET_p and annual ET_p for each subbasin is then calculated as the arithmetic mean of ET_p of the selected COOP stations.

[14] Because the purpose of our study is to examine the impact of runoff generation mechanisms (e.g., baseflow vs. overland flow) on basin water balance in relation to soil texture, a hydrologic measure is needed to diagnose the difference in the forms of streamflow generation. If a streamflow hydrograph is conceptualized as the aggregate of baseflow (i.e., release of groundwater storage) and quickflow (e.g., direct response to rainfall events), then in the absence of detailed field observations, the contribution of groundwater to streamflow can be approximated by a baseflow index (BFI: baseflow-to-streamflow ratio). A range of techniques have been developed for calculating BFI [*Hall*, 1968; *Smakhtin*, 2001]. Here, BFI is approximated using a recursive digital filter [*Nathan and McMahon*, 1990; *Chapman*, 1991] as:

$$Q_b(i) = kQ_b(i-1) + \frac{1-k}{2}[Q(i) + Q(i-1)] \quad (7)$$

where i is an index of day, k is a filter parameter, and Q and Q_b are the measured daily streamflow rate and estimated baseflow rate at day i, respectively. This digital filter, commonly used in signal analysis and processing, can remove high-frequency quickflow signals from the hydrograph to derive low-frequency baseflow signals [*Nathan and McMahon*, 1990; *Chapman*, 1991]. By studying 141 gauging stations, *Szilagyi et al.* [2003] suggested an optimized value of 0.93 for the filter parameter k in the study area. With the rate of baseflow estimated from equation (7), the long-term BFI (BFI = $\sum_{i=1}^{n} Q_b / \sum_{i=1}^{n} Q$, where n is the total number of days of available streamflow records) is used in this study [*Szilagyi et al.*, 2003].

[15] There is some limited use of water for irrigation in the study area. To evaluate the impact of irrigation on streamflow, we obtained surface water diversion data from the Nebraska Department of Natural Resources (http://dnrdata.dnr.ne.gov/shifts/stream.asp). In each subbasin, we developed time series of runoff equivalent of surface water diversion by dividing the total irrigation water diverted in a subbasin by the subbasin drainage area. The analyses described below in section 4 were repeated by adding the diverted water back to the observed runoff to represent "unmanaged" conditions. However, we found that water diversions from the rivers are limited in this region and the general findings of this paper are not affected by neglecting surface diversions. Therefore, we present our analysis directly using the streamflow gauge data without any further manipulations.

4. Results and Discussions

4.1. Impact of Soil Texture on Mean Annual Water Balance

[16] The long-term mean annual runoff ($\overline{R}$), precipitation ($\overline{P}$), aridity index ($\overline{\Phi}$), and baseflow index (BFI) of the 34 subbasins are reported in Table 2. In the region, $\overline{P}$ increases from about 400 mm/a in the western Niobrara River basin to over 700 mm/a in the eastern Elkhorn River basins, while $\overline{ET_p}$ decreases in the same direction [*Szilagyi et al.*, 2005]. As a result, $\overline{\Phi}$ grows from east to west (Table 2). To examine the impact of the Sand Hills on runoff generation, the relationship between $\overline{R}$ and $\overline{P}$ of the studied subbasins is

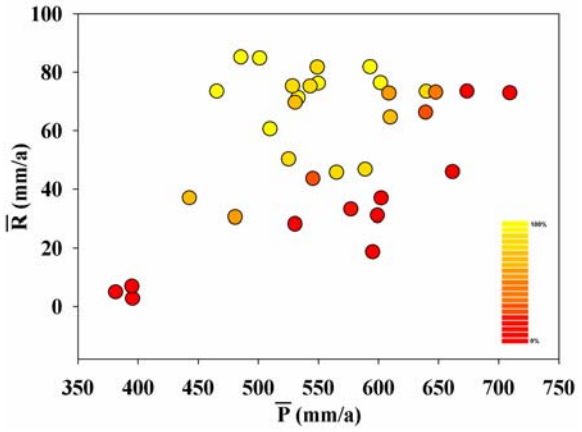

Figure 3. Relationship between long-term mean annual precipitation ($\overline{P}$) and runoff ($\overline{R}$) for the 34 selected subbasins. Color gradient, yellow (100%)-to-red (0%), reflects the Sand Hills coverage in the subbasins.

plotted in Figure 3. Three data points with the lowest $\overline{P}$ and $\overline{R}$ in Figure 3 correspond to the subbasins located in the headwaters of the Niobrara River (e.g., N2, N7, and N8) in the western edge of the study area. Figure 3 reveals that under a similar range of $\overline{P}$, the basins in the Sand Hills exhibit much higher $\overline{R}$ than those outside of the Sand Hills (Table 2). This signifies the impact of the Sand Hills on mean annual runoff.

[17] A higher $\overline{R}$ suggests a lower $(\overline{P} - \overline{R})$ under the same $\overline{P}$. In Figure 4, $(\overline{P} - \overline{R})/\overline{P}$ and $\overline{\Phi}$ of each subbasin are plotted along with a family of $\overline{ET}_a/\overline{P}$ vs. $\overline{\Phi}$ curves from equation (3). Three sets of $\overline{\Phi}$ values are used in Figure 4. The first set of $\overline{\Phi}$ (hereafter designated as $\overline{\Phi}_1$) is directly calculated using the Priestley-Taylor equation-based ET_p from the AWDN stations, and P from the PRISM data set for each subbasin, whenever the time periods of calculated ET_p and streamflow data overlap (Figure 4a). This results in 31 subbasins with a minimum of 10- and a maximum of 25-year data. Three subbasins are omitted from Figure 4a due to no overlapping periods of net radiation and streamflow data. The second set of $\overline{\Phi}$ (hereafter designated as $\overline{\Phi}_2$) is estimated from precipitation using the empirical power functions explained above (equation (5); Figure 4b). The last set of $\overline{\Phi}$ (hereafter designated as $\overline{\Phi}_3$) is calculated using ET_p, estimated by the Hargreaves equation using data from the COOP stations, and P from the PRISM data set for each subbasin (Figure 4c). Note that for some subbasins in Figure 4, the values of $(\overline{P} - \overline{R})/\overline{P}$ are slightly different because of the different periods used for calculating water balance. We found that annual ET_p estimated by the Hargreaves equation is about several hundred millimeters lower than the one estimated by the Priestley-Taylor equation, while the Priestley-Taylor equation-based estimates are in good agreement with those reported by *Szilagyi et al.* [2005] in this region. As a result, $\overline{\Phi}_1$ and $\overline{\Phi}_2$ (Figures 4a and 4b) are higher than $\overline{\Phi}_3$ (Figure 4c). Also using the Hargreaves equation, *Vogel and Sankarasubramanian* [2005] reported similar $\overline{\Phi}$ values to $\overline{\Phi}_3$. *Zhang et al.* [2001] also noticed that the results may vary because of the different methods employed to calculate ET_p. Despite the differences in $\overline{\Phi}$, the purpose of our study is to qualitatively discern the impacts of groundwater and soil texture on basin water balance. Overall, the results exhibit a similar pattern with the Sand Hills proportions in the subbasins designated by a gradient of marker colors (Figures 4a, 4b, and 4c). However, for the purpose of prediction (e.g., runoff), careful selection of ET_p equations is necessary for using equation (3), as w value may vary depending on the results of ET_p.

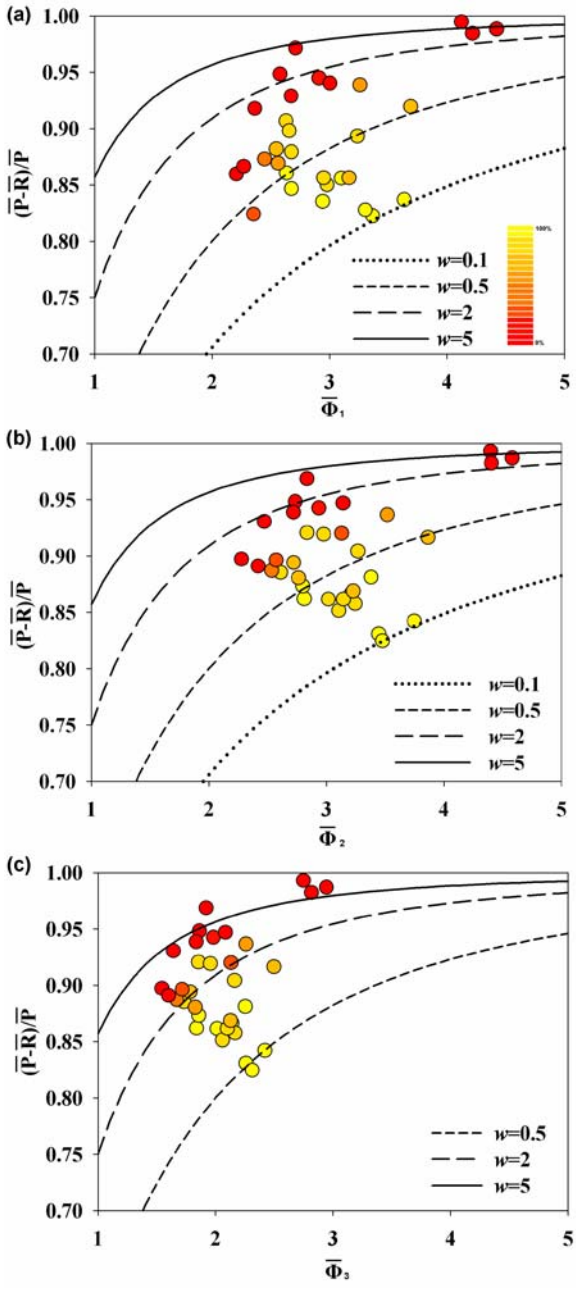

Figure 4. Relationship between estimated long-term mean annual $(\overline{P} - \overline{R})/\overline{P}$ and aridity index ($\overline{\Phi}$) calculated based on (a) the Priestley-Taylor equation-based ET_p and P obtained from the PRISM data set, (b) power functions of equation (5) and P obtained from the PRISM data set, and (c) the Hargreaves equation-based ET_p and P obtained from the PRISM data set. Equation (3) from the work of *Zhang et al.* [2001] is plotted with w = 0.1, 0.5, 2.0, and 5.0, respectively. Color gradient, yellow (100%)-to-red (0%), reflects the Sand Hills coverage in the subbasins.

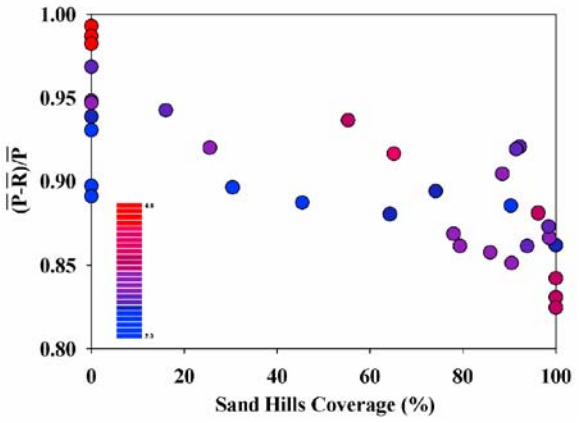

Figure 5. Relationship between $(\overline{P} - \overline{R}) / \overline{P}$ and the Sand Hills coverage for each subbasin. Color gradient, blue-to-red, designates climate transition from wet to dry.

[18] In earlier studies, the differences in $(\overline{P} - \overline{R})/\overline{P}$ values for a given $\overline{\Phi}$ were shown to reflect the influence of climate and basin properties (e.g., climate seasonality, soil, and vegetation) on water balance [*Milly*, 1994; *Koster and Suarez*, 1999; *Zhang et al.*, 2001; *Porporato et al.*, 2004; *Yokoo et al.*, 2008]. *Zhang et al.* [2001] suggested optimized values of $w = 0.5$ and $w = 2$ for grasslands and forests, respectively. It is important to note here that despite a fourfold difference between the two optimized w values, $(\overline{P} - \overline{R})/\overline{P}$ vs. $\overline{\Phi}$ pairs reported by *Zhang et al.* [2001] were highly scattered with a significant mixture of forested and grassed basins under similar aridity indices. *Zhang et al.* [2001] used $w = 0.1$ to bound their lower $(\overline{P} - \overline{R})/\overline{P}$ and a 1:1 line ($(\overline{P} - \overline{R})/\overline{P} = \overline{\Phi}$) to bound the higher $(\overline{P} - \overline{R})/\overline{P}$ values. Although our $(\overline{P} - \overline{R})/\overline{P}$ vs. $\overline{\Phi}$ data as a whole do not follow the Budyko hypothesis, the data, when distinguished according to Sand Hills coverage, show some relationships. With the aid of equation (3), the impact of the Sand Hills on basin water balance can be distinguished. As expected from Figure 3, Figure 4 shows that for a given $\overline{\Phi}$, the subbasins that are fully located in the Sand Hills have the lowest $(\overline{P} - \overline{R})/\overline{P}$ values (in bright yellow color); whereas, the subbasins that are completely outside the Sand Hills have the highest $(\overline{P} - \overline{R})/\overline{P}$ values (in red color) and exhibit a pervasive trend along a range of aridity indices, underscoring the significance of climatic controls on mean annual water balance when soil textures are finer. Meanwhile, the subbasins that are partially located in the Sand Hills have intermediate $(\overline{P} - \overline{R})/\overline{P}$ values. Figure 4 strongly suggests the control of sandy soils on the partitioning of precipitation into basin runoff and evapotranspiration. When the data are grouped as a whole without considering soil textural differences, there is no clear positive trend between aridity index and evapotranspiration ratio. This suggests that soil textural differences among the subbasins can strongly modify the impact of climate on regional water balance.

[19] To further explore the impact of the Sand Hills on basin water balance, the $(\overline{P} - \overline{R})/\overline{P}$ ratio is plotted against the Sand Hills coverage for each subbasin in Figure 5. Note that in Figure 5, marker colors illustrate the aridity index with a gradient of blue (wet) to red (dry). With increasing areal coverage of the Sand Hills in the subbasins, the $(\overline{P} - \overline{R})/\overline{P}$ ratio decreases significantly (Figure 5). Besides this direct control of soil texture, the impact of soil in mediating the role of climate in water balance may be teased out in Figure 5. If the impact of climate is equally pervasive independent of soil texture, then the blue-to-red color transition would occur in the vertical direction from low to high $(\overline{P} - \overline{R})/\overline{P}$ as climate becomes more arid. This is clearly observed for subbasins outside the Sand Hills plotted in the left-end, and to some extent in the mid section of Figure 5. However, with the Sand Hills coverage exceeding ~75–80%, marker colors blend each other without a clear vertical transition. This may suggest that the impact of soils could outweigh the impact of climate control in the subbasins underlain by coarse materials. However, for the subbasins that are completely inside the Sand Hills, climate controls on mean annual water balance becomes clear, as the $(\overline{P} - \overline{R})/\overline{P}$ ratio is lower for the subbasins with wetter climatic conditions and higher for drier climatic conditions (e.g., right-end members in Figure 5).

[20] Next, we illustrate the impact of both climate and soil texture gradients along the Niobrara River, by plotting $\overline{R}/\overline{P}$ and $\overline{\Phi}_2$ for the subbasins along the mainstream of the river in the direction from west to east (Figure 6). For the purpose of clarity and simplicity, $\overline{\Phi}_1$ and $\overline{\Phi}_3$ are not plotted in Figure 6, as they exhibit the same pattern as does $\overline{\Phi}_2$. The subbasins in the middle portion of this transect are located in the Sand Hills with varying fractions of Sand Hills coverage (e.g., N1, N4, N5, and N10), while the rest of the subbasins are located outside the Sand Hills (i.e., N2, N3, N6, N7, N8, and N9). As a result of an increasing trend in $\overline{P}$, $\overline{\Phi}_2$ decreases from 4.5 in the west to 2.7 in the east. Given that other conditions remain similar, this west-east decrease in $\overline{\Phi}_2$ would lead to, on the basis of the Budyko hypothesis, a west-east increase in $\overline{R}/\overline{P}$. As expected, such an increase is clear in the data (Figure 6). However, superimposed on this increasing trend, the subbasins in the Sand Hills show remarkably higher $\overline{R}/\overline{P}$ ratios. For example, $\overline{R}/\overline{P}$ in the subbasin N5 is 9 times as high as in the neighboring subbasin N8.

[21] The results indicate that the Nebraska Sand Hills has a significant impact on mean annual basin water balance in the region (Figures 3, 4, 5, and 6). Given the same climatic conditions (e.g., $\overline{P}$ and $\overline{\Phi}$), the subbasins that are either fully or partially located in the Sand Hills exhibit higher $\overline{R}/\overline{P}$ ratios and consequently lower $(\overline{P} - \overline{R})/\overline{P}$ ratios. *Zhang et al.* [2001] attributed the differences in evapotranspiration and runoff ratios under the same aridity index to land cover conditions. Furthermore, *Milly* [1994] showed the impact of soil texture on the Budyko curve. Following those earlier studies, the observed higher $\overline{R}/\overline{P}$ ratios in the Sand Hills subbasins could either be a result of sparser vegetation cover or shorter residence time of soil moisture within the root zone in coarser soils (e.g., higher groundwater recharge), or both, as the selected subbasins exhibit similar climate seasonality (Figure 2).

[22] The study area is largely treeless [*Bleed and Flowerday*, 1989] and the vegetation cover is predominantly composed of native warm C4 grasses. Interbasin differences in land cover are relatively small [*Dappen et al.*, 2007], while soil textures are remarkably different between the Sand Hills (mainly eolian sand deposits) and adjacent subbasins (mainly less permeable silt loam; Table 1).

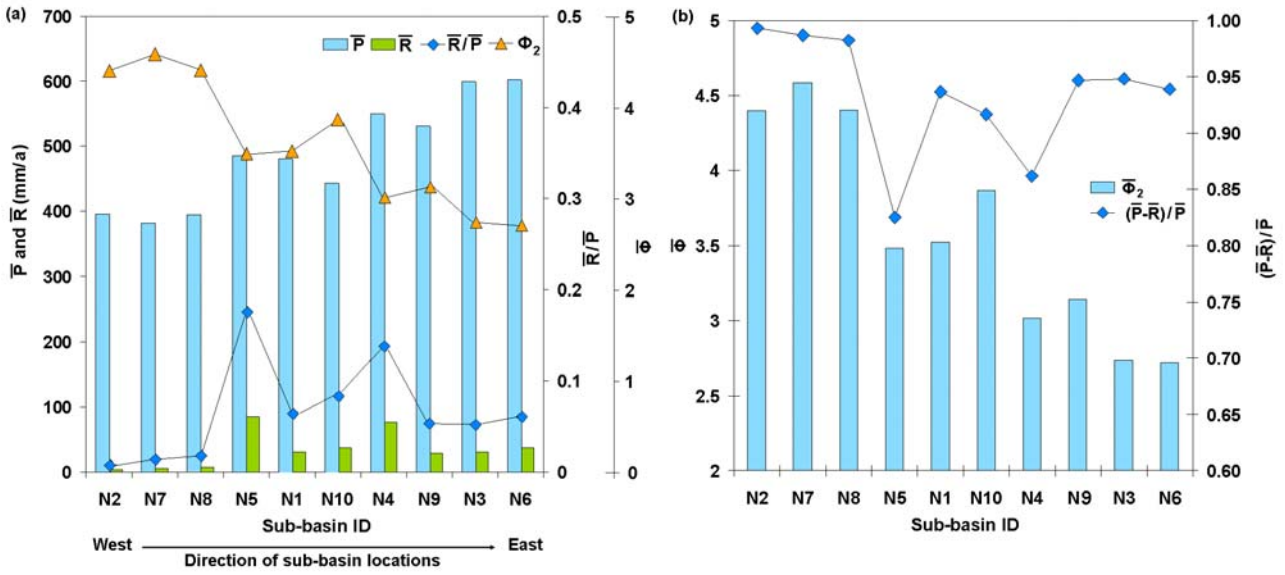

Figure 6. Long-term mean annual precipitation ($\overline{P}$), runoff ($\overline{R}$), aridity index ($\overline{\Phi}_2$), $\overline{R}$ / $\overline{P}$, and ($\overline{P} - \overline{R}$) / $\overline{P}$ of the subbasins located in the Niobrara River Basin. The direction is along the flowing direction of the Niobrara River from (left) the west to (right) the east.

According to the class-averaged values [*Schaap et al.*, 1998], the saturated hydraulic conductivity of sand is about one order of magnitude larger than that of silt loam. In a Sand Hills field study, *Wang et al.* [2008, 2009b] measured saturated hydraulic conductivity of vadose zone ranging between 200 and 1500 cm/day, which is significantly higher than the class-averaged value of ~18 cm/day with a range between 3 and 100 cm/day for silt loam [*Schaap et al.*, 1998]. Therefore, we suggest that soil textural differences play an important role in determining the water balance across the region. As discussed previously, coarser soils produce more groundwater recharge (and usually less surface runoff) under similar climatic and vegetation conditions, mainly due to less residence time of soil moisture within the root zone for evapotranspiration [*De Vries and Simmers*, 2002; *Small*, 2005; *Wang et al.*, 2009a]. The infiltrated water reaches the groundwater table, travels across the basin, and forms the baseflow. As such, under similar climatic and vegetation conditions, a basin with a higher groundwater recharge would be expected to have both a higher BFI and $\overline{R}/\overline{P}$. Consistent with this explanation, Figure 7 interestingly shows that the Sand Hills subbasins exhibit both higher BFIs and $\overline{R}/\overline{P}$ ratios. On the contrary, three subbasins in Figure 7 also show high BFIs but very low $\overline{R}/\overline{P}$ ratios. These subbasins are located in the western edge of the study area where soil is finer and climate is much drier. Despite stream discharge is maintained by baseflow (i.e., high BFI) in this region, low rates of groundwater recharge lead to lower $\overline{R}/\overline{P}$ ratios [*Brunke and Gonser*, 1997]. As such, we interpret this observation of higher BFIs and $\overline{R}/\overline{P}$ ratios in the Sand Hills subbasins as strong evidence of higher groundwater recharge. In a vadose zone modeling study, *Wang et al.* [2009a] found 2 to 10 times higher rates of groundwater recharge produced by sandy soils with respect to finer soil textures in the Sand Hills.

[23] In summary, under the same seasonal climate behavior, we attribute the observed differences in the mean annual water balance between the Sand Hills and non-Sand Hills subbasins mainly to variations in the soil texture among the subbasins. The rapid deep percolation of soil moisture in the Sand Hills basins limits evapotranspiration, recharges groundwater, promotes baseflow, and ultimately leads to higher runoff. We argue that the higher $\overline{R}/\overline{P}$ ratio in the Sand Hills subbasins represents the missed opportunity for evapotranspiration, rather than convergence of regional groundwater into those subbasins. This interpretation is consistent with regional groundwater maps showing that the groundwater table divides follow the topographic boundaries of the subbasins and elevations of groundwater tables in the Sand Hills are generally higher compared to the adjacent regions. If other conditions remain similar, basins covered by coarser soils tend to have lower ($\overline{P} - \overline{R}$)/$\overline{P}$ ratios, which can be predicted by using a lower w value in equation (3). However, this conclusion may not hold for regions where

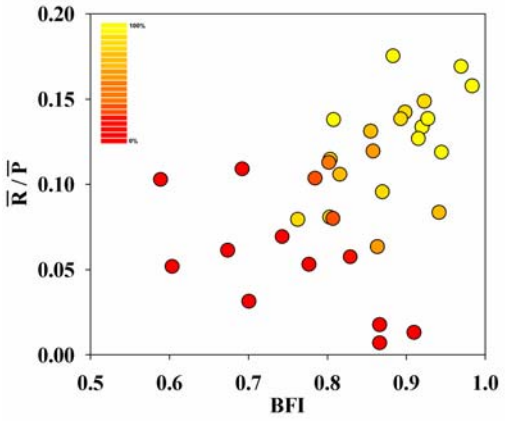

Figure 7. Relationship between baseflow index (BFI) and long-term mean annual $\overline{R}/\overline{P}$ of the 34 subbasins. Color gradient, yellow (100%)-to-red (0%), reflects the Sand Hills coverage in the subbasins.

streams lose water to groundwater on an annual basis (i.e., the elevation of the groundwater table is below the elevation of the streambed).

4.2. Impact of Baseflow on Interannual Water Balance

[24] The Budyko hypothesis implies that the long-term change in basin water storage is negligible. However, to assess the temporal scales over which this assumption may hold is not trivial. Based on the assumption that the interannual change in basin water storage is much smaller than evapotranspiration and runoff, the Budyko hypothesis has been extended to study interannual variability in basin water balance [*Koster and Suarez*, 1999; *Arora*, 2002; *Zhang et al.*, 2008]. Recently, *Zhang et al.* [2008] predicted daily, monthly, annual, and long-term mean annual streamflow using Budyko-type equations. *Zhang et al.* [2008] showed good agreement between the observed and predicted annual streamflow in some basins, but their model did poorly in others. It is thus critical to understand the basin hydrologic conditions that support the Budyko hypothesis at various temporal scales for the future use of this model. This is particularly important in baseflow-dominated basins, which may show little interannual variability in streamflow, as groundwater moves at a much slower velocity than overland flow, filtering out the interannual variability in precipitation. *Bentall* [1989] noted remarkably steady rates of streamflow in the rivers originating from the Sand Hills. For example, the ratio of maximum to minimum mean monthly discharge is only 1.19 for the Dismal River (L4), while in a neighboring stream this ratio is 2.71 (Mud Creek, L2). Here, we examine the impact of baseflow on the annual water balance as well as its implications for the Budyko curve.

[25] To investigate the impact of baseflow on the annual basin water balance, we examine annual runoff-precipitation and $(P - R)/P$ vs. Φ relations of four subbasins characterized within a narrow range of $(\overline{P} - \overline{R})/\overline{P}$ and $\overline{\Phi}$, but with considerably different BFIs. The narrow range of $(\overline{P} - \overline{R})/\overline{P}$ and $\overline{\Phi}$ of the four subbasins suggest that they behave almost identically over mean annual time scales, and therefore any differences in their annual water balance may be attributed to the difference in baseflow contributions. These include the subbasin L7, L5, E8, and E2, with the BFI value decreasing in the respective order. Among these subbasins, $\overline{\Phi}$ of L7 is slightly larger than the others. The annual $P - R$ and $(P - R)/P$ vs. Φ data, including $\overline{\Phi}_2$ and $\overline{\Phi}_3$, of the four subbasins are plotted in Figure 8. Despite the differences in Φ values due to different equations used for calculating ET_p, the overall patterns stay the same for each individual subbasin. Strikingly, Figure 8 shows notable differences in the annual runoff response to precipitation for the four subbasins. Most significantly, the annual runoff of L7 with the highest BFI has a nearly constant rate. Despite a more than twofold increase in annual precipitation from 270 to 720 mm/a, the annual R only shows subtle fluctuations by 30% (Figure 8a). As the BFI gets smaller for the other three subbasins, a positive correlation between R and P gradually emerges, despite a significant scatter in the observed data, which might be caused by interannual differences in seasonal rainfall totals and rainfall intensity (Figures 8d, 8g, and 8j). For the end-member E2 with BFI = 0.59, annual R varies by over one order of magnitude from merely 5 to more than 250 mm/a; while annual P ranges from approximately 400 to 1000 mm/a. In the Sand Hills subbasins, the high infiltration capacity of sandy soils limits overland flow, increases BFI, and modulates basin runoff response to interannual variations in precipitation. With increasing BFI, groundwater storage-release processes gradually dominate runoff generation and buffer the system from fluctuations in annual P. As such, the larger the BFI, the steadier the system is in terms of precipitation-runoff response.

[26] The various degrees of sensitivity of basin annual runoff to precipitation lead to considerably different patterns of $(P - R)/P$ vs. Φ relations (Figures 8b, 8c, 8e, 8f, 8h, 8i, 8k, and 8l). Interestingly in L7, $(P - R)/P$ is negatively related to annual Φ. As the BFI decreases, this negative relationship gradually transits into a positive one (Figures 8h, 8i, 8k, and 8l), which is in general agreement with the trend predicted by equation (3). Strictly speaking, when the interannual change in basin water storage is negligible, a negative $(P - R)/P$ vs. Φ trend (as in L7 and L5) would suggest smaller $(P - R)/P$ ratios in drier years (e.g., $P < \overline{P}$) as compared to the Budyko hypothesis. However, the dominance of baseflow in annual runoff and the lack of dependence of annual runoff on precipitation in L7 and L5 imply a longer-term (at least more than a year) hydrologic memory in those basins. This indicates that the impact of change in water storage cannot be neglected in the Sand Hills basins for estimating annual runoff using equation (3). An explanation for the observed negative $(P - R)/P$ vs. Φ trend may be given as follows. When runoff is dominated by baseflow, the majority of basin runoff observed in a dry year is released from the groundwater storage in the basin (e.g., old water stored from previous years). When the source of runoff is considered to be solely from annual precipitation by neglecting the contribution of the old water in the system, the ''actual evapotranspiration'' calculated as a closure in water balance underestimates the basin evapotranspiration. This underestimation increases as annual climate (e.g., Φ) gets drier. In the case when baseflow contribution is significant, the ratio of ET_a/P can be written by including a storage term (ΔS) to close the water balance:

$$\frac{ET_a}{P} = \frac{P - R}{P} - \frac{\Delta S}{P} = F(\Phi) \tag{8}$$

When the deep percolation to the groundwater table is less than the release of baseflow, ΔS is negative. As a result, neglecting the storage term in equation (8) would lead to an underestimation of ET_a/P, and therefore $ET_a/P < F(\Phi)$. When deep percolation is higher than the release of baseflow, ΔS is positive, and neglecting the storage term in equation (8) would lead to an overestimation of ET_a/P in comparison to the Budyko hypothesis. In summary, for subbasins within a similar range of $(\overline{P} - \overline{R})/\overline{P}$ and $\overline{\Phi}$, the annual R-P and $(P - R)/P$ vs. Φ relationships exhibit considerably different patterns depending on BFI. The baseflow-dominated basins exhibit a negative relationship between annual $(P - R)/P$ and Φ; whereas, with decreasing BFI, this negative relationship gradually transits into a weak positive relationship that follows the Budyko hypothesis.

5. Conclusions

[27] In this study, we examined and compared the long-term mean annual and interannual water balance of basins located within and around the Nebraska Sand Hills, the

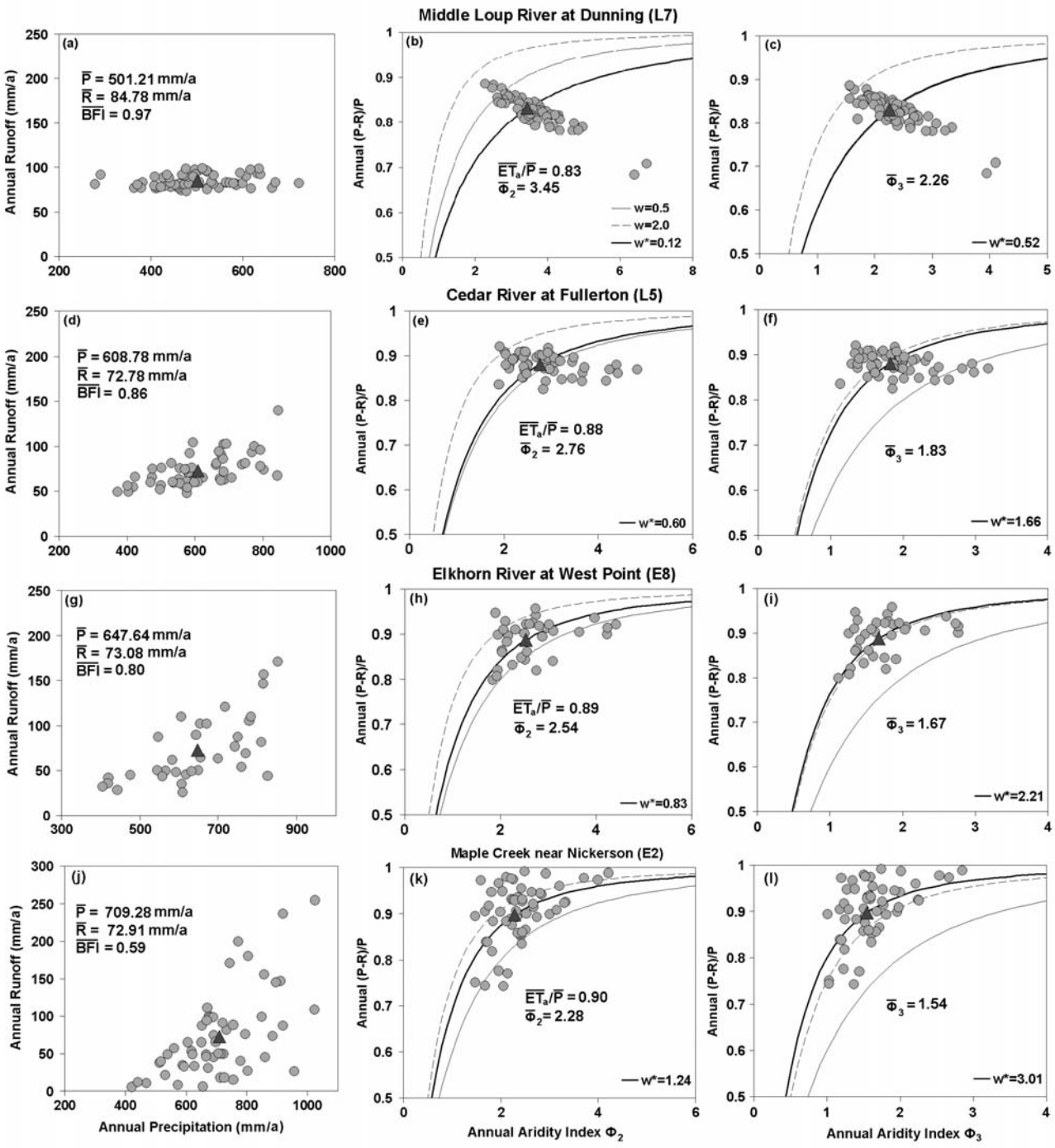

Figure 8. Relationships between annual precipitation (P) and runoff (R) and between annual aridity index (Φ) and $(P - R)/P$ among the four selected subbasins. Darker triangles are the long-term means, and w^* is the calibrated value of w in equation (3) for each subbasin using the entire available records.

largest grassland-stabilized sand dune field in the Western Hemisphere. Among the basins studied, soil texture varies remarkably from sand in the Sand Hills to mainly silt loam outside of the Sand Hills, while vegetation cover remains relatively similar. The Budyko hypothesis is used as a diagnostic tool to evaluate the role of soil texture and groundwater on both long-term mean annual and interannual water balances. A baseflow index is used as additional information to aid in the interpretation of precipitation and runoff data.

[28] Overall, our results underscore a significant impact of soil texture on regional hydrology. On long-term mean annual time scales, the Sand Hills basins generate more runoff than those outside of the Sand Hills (particularly relative to the amount of received precipitation). The higher BFI of the Sand Hills basins and the positive correlation between BFI and $\overline{R}/\overline{P}$ indicate a close tie between runoff and groundwater recharge. Given that the groundwater table divides follow the topographic boundaries in the region and elevations of groundwater tables in the Sand Hills are

generally higher, our results imply that the highly permeable sandy soils of the Sand Hills basins result in reduced actual evapotranspiration and thus higher $\overline{R}$. A Budyko-type relationship is observed when the subbasins are grouped according to soil texture. However, no clear positive relationship exists between $\overline{\Phi}$ and $(\overline{P} - \overline{R})/\overline{P}$ for the data as a whole. On annual time scales, the differences in the annual *R-P* relationship reflect the impacts of soil texture and groundwater on the regional water balance. For subbasins within a similar range of $(\overline{P} - \overline{R})/\overline{P}$ and $\overline{\Phi}$, the annual *R-P* and $(P - R)/P$ vs. Φ relationships exhibit considerably different patterns depending on BFI. The baseflow-dominated basins exhibit a negative relationship between annual $(P - R)/P$ and Φ, which deviates from the original Budyko hypothesis. This is because baseflow is much steadier than quickflow in response to interannual changes in precipitation, and the interannual change in basin water storage is not negligible. However, with decreasing BFI, this negative relationship gradually transits into a weak positive relationship that follows the Budyko hypothesis.

[29] Our results have important implications for modeling land surface-atmosphere interactions. We found that on long-term mean annual time scales, basins covered by coarser soils tend to have lower representative *w* values in the equation proposed by *Zhang et al.* [2001]. In addition to modeling water yield in ungauged basins, this observation is crucial for studying impacts on the regional climate, as lower latent heat resulting from a lower actual evapotranspiration-to-precipitation ratio may lead to higher sensible heat flux and thus elevated surface temperature [*Maxwell and Kollet*, 2008]. In large areas this may impact regional weather patterns. As far as our analysis is concerned, the sensitivity of annual basin runoff to climatic fluctuations reduces with increasing BFI. This may have important implications for managing water resources under a fluctuating climate. Future work will need to consider the role of the frequency and magnitude of climate fluctuations.

[30] **Acknowledgments.** We thank two anonymous reviewers, whose comments have greatly improved the paper. The research reported herein was supported in part by the Nebraska Department of Natural Resources-Nebraska Environmental Trust (Project 08-141-2), the University of Nebraska Water Center as well as the Rural Initiative.

References

Arora, V. K. (2002), The use of the aridity index to assess climate change effect on annual runoff, *J. Hydrol.*, *265*, 164–177.

Atkinson, S. E., R. A. Woods, and M. Sivapalan (2002), Climate and landscape controls on water balance model complexity over changing timescales, *Water Resour. Res.*, *38*(12), 1314, doi:10.1029/2002WR001487.

Bentall, R. (1989), Streams, in *An Atlas of the Sand Hills*, edited by A. Bleed and C. Flowerday, Conservation and Survey Division, University of Nebraska, Lincoln, Nebraska, Resource Atlas No. 5a, pp. 93–114.

Bleed, A., and C. Flowerday (1989), *An Atlas of the Sand Hills*, Conservation and Survey Division, University of Nebraska, Lincoln, Nebraska, Resource Atlas No. 5a.

Brunke, M., and T. Gonser (1997), The ecological significance of exchange processes between rivers and ground-water, *Freshwater Biol.*, *37*, 1–33.

Brutsaert, W. (2008), Long-term groundwater storage trends estimated from streamflow records: Climatic perspective, *Water Resour. Res.*, *44*, W02409, doi:10.1029/2007WR006518.

Brutsaert, W., and J. L. Nieber (1977), Regionalized drought flow hydrographs from a mature glaciated plateau, *Water Resour. Res.*, *13*, 637–643.

Budyko, M. I. (1958), *The Heat Balance of the Earth's Surface*, 259 pp., U.S. Dept. of Commerce, Washington, D. C.

Budyko, M. I. (1974), *Climate and Life*, 508 pp., Academic Press, New York.

Chapman, T. (1991), Comment on "Evaluation of automated techniques for base flow and recession analyses" by R. J. Nathan and T. A. McMahon, *Water Resour. Res.*, *27*, 1783–1784.

Chen, X., X. H. Chen, C. Rowe, Q. Hu, and M. Anderson (2003), Geological and climatic controls on streamflows in the Nebraska Sand Hills, *J. Am. Water Resour. Assoc.*, *39*, 217–228.

Choudhury, B. J. (1999), Evaluation of an empirical equation for annual evaporation using field observations and results from a biophysical model, *J. Hydrol.*, *216*, 99–110.

Daly, C., R. P. Neilson, and D. L. Phillips (1994), A statistical topographic model for mapping climatological precipitation over mountain terrain, *J. Appl. Meteorol.*, *33*, 140–158.

Daly, C., W. P. Gibson, G. H. Taylor, G. L. Johnson, and P. Pasteris (2002), A knowledge-based approach to the statistical mapping of climate, *Clim. Res.*, *22*, 99–113.

Dappen, P., J. Merchant, I. Ratcliffe, and C. Robbins (2007), *Delineation of 2005 Land Use Patterns for the State of Nebraska*, Nebraska Dept. of Natural Resources, Lincoln, N. Engl. (Available at http://www.dnr.state.ne.us/docs/studiesandresearch.html)

De Vries, J. J., and I. Simmers (2002), Groundwater recharge: An overview of processes and challenges, *Hydrogeol. J.*, *10*, 5–17.

Farmer, D., M. Sivapalan, and C. Jothityangkoon (2003), Climate, soil, and vegetation controls upon the variability of the water balance in temperate and semiarid landscapes: Downward approach to water balance analysis, *Water Resour. Res.*, *39*(2), 1035, doi:10.1029/2001WR000328.

Hall, F. R. (1968), Base flow recessions: A review, *Water Resour. Res.*, *4*, 973–983.

Hargreaves, G. L., and Z. A. Samani (1982), Estimating potential evapotranspiration, *J. Irrig. Drain. Eng., ASCE*, *108*, 225–230.

Koster, R. D., and M. J. Suarez (1999), A simple framework for examining the interannual variability of land surface moisture fluxes, *J. Clim.*, *12*, 1911–1917.

Loope, D., and J. Swinehart (2000), Thinking like a dune field: Geologic history in the Nebraska Sand Hills, *Great Plains Res.*, *10*, 5–35.

Marani, M., E. Eltahir, and A. Rinaldo (2001), Geomorphic controls on regional base flow, *Water Resour. Res.*, *37*, 2619–2630.

Maxwell, R. M., and S. J. Kollet (2008), Interdependence of groundwater dynamics and land-energy feedbacks under climate change, *Nat. Geosci.*, *1*, 665–669, doi:10.1038/ngeo315.

McGuire, V. L., and B. C. Fischer (1999), Water-level changes, 1980 to 1997, and saturated thickness, 1996 to 97, in the High Plains Aquifer, *U.S. Geological Survey Fact Sheet, FS-124-99*.

Milly, P. C. (1994), Climate, soil water storage, and the average annual water balance, *Water Resour. Res.*, *30*, 2143–2156.

Milly, P. C., and K. A. Dunne (2002), Macroscale water fluxes: 2. Water and energy supply control of their interannual variability, *Water Resour. Res.*, *38*(10), 1206, doi:10.1029/2001WR000760.

Nathan, R. J., and T. A. McMahon (1990), Evaluation of automated techniques for base flow and recession analyses, *Water Resour. Res.*, *26*, 1465–1473.

Porporato, A., E. Daly, and I. Rodriguez-Iturbe (2004), Soil water balance and ecosystem response to climate change, *Am. Nat.*, *164*(5), 625–632.

Priestley, C. H. B., and R. J. Taylor (1972), On the assessment of surface heat flux and evaporation using large-scale parameters, *Mon. Weather Rev.*, *100*, 81–82.

Rodriguez-Iturbe, I., and A. Porporato (2004), *Ecohydrology of Water Controlled Ecosystems: Soil Moisture and Plant Dynamics*, 442 pp., Cambridge Univ. Press, Cambridge, U. K.

Sankarasubramanian, A., and R. M. Vogel (2002), Annual hydroclimatology of the United States, *Water Resour. Res.*, *38*(6), 1083, doi:10.1029/2001WR000619.

Sankarasubramanian, A., R. M. Vogel, and J. F. Limbrunner (2001), Climate elasticity of streamflow in the United States, *Water Resour. Res.*, *37*, 1771–1781.

Schaap, M. G., F. J. Leij, and M. T. van Genuchten (1998), Neural network analysis for hierarchical prediction of soil hydraulic properties, *Soil Sci. Soc. Am. J.*, *62*, 847–855.

Smakhtin, V. U. (2001), Low flow hydrology: A review, *J. Hydrol.*, *240*, 147–186.

Small, E. E. (2005), Climatic controls on diffuse groundwater recharge in semiarid environments of the southwestern United States, *Water Resour. Res.*, *41*, W04012, doi:10.1029/2004WR003193.

Szilagyi, J., E. F. Harvey, and J. F. Ayers (2003), Regional estimation of base recharge to ground water using water balance and a base-flow index, *Ground Water*, *41*, 504–513.

Szilagyi, J., E. F. Harvey, and J. F. Ayers (2005), Regional estimation of total recharge to ground water in Nebraska, *Ground Water*, *43*, 63–69.

Vogel, R. M., and A. Sankarasubramanian (2005), *USGS Hydro-Climatic Data Network (HCDN): Monthly Climate Database, 1951–1990*, Oak Ridge National Laboratory Distributed Active Archive Center, Oak Ridge, Tenn., doi:10.3334/ORNLDAAC/810.

Wagener, T., M. Sivapalan, P. Troch, and R. Woods (2007), Catchment classification and hydrologic similarity, *Geogr. Compass*, *1*, 901–931.

Wang, T., V. A. Zlotnik, D. Wedin, and K. D. Wally (2008), Spatial trends in saturated hydraulic conductivity of vegetated dunes in the Nebraska Sand Hills: Effects of depth and topography, *J. Hydrol.*, *349*, 88–97.

Wang, T., V. A. Zlotnik, J. Simunek, and M. G. Schaap (2009a), Using pedotransfer functions in vadose zone models for estimating groundwater recharge in semiarid regions, *Water Resour. Res.*, *45*, W04412, doi:10.1029/2008WR006903.

Wang, T., D. Wedin, and V. A. Zlotnik (2009b), Field evidence of a negative correlation between saturated hydraulic conductivity and soil carbon in a sandy soil, *Water Resour. Res.*, *45*, W07503, doi:10.1029/2008WR006865.

Williams, C. A., and J. D. Albertson (2005), Contrasting short- and long-timescale effects of vegetation dynamics on water and carbon fluxes in water-limited ecosystems, *Water Resour. Res.*, *41*, W06005, doi:10.1029/2004WR003750.

Yokoo, Y., M. Sivapalan, and T. Oki (2008), Investigating the roles of climate seasonality and landscape characteristics on mean annual and monthly water balances, *J. Hydrol.*, *357*, 255–269.

Zhang, L., W. R. Dawes, and G. R. Walker (2001), Response of mean annual evapotranspiration to vegetation changes at basin scale, *Water Resour. Res.*, *37*, 701–708.

Zhang, L., K. Hickel, W. R. Dawes, F. H. S. Chiew, A. W. Western, and P. R. Briggs (2004), A rational function approach for estimating mean annual evapotranspiration, *Water Resour. Res.*, *40*, W02502, doi:10.1029/2003WR002710.

Zhang, L., N. Potter, K. Hickel, Y. Zhang, and Q. Shao (2008), Water balance modeling over variable time scales based on the Budyko framework — model development and testing, *J. Hydrol.*, *360*, 117–131.

E. Istanbulluoglu, Department of Civil and Environmental Engineering, University of Washington, More Hall, Seattle, WA 98195, USA. (erkani@u.washington.edu)

J. Lenters, and T. Wang, School of Natural Resources, University of Nebraska, 521 Hardin Hall, Lincoln, NE 68583, USA. (jlenters2@unl.edu; twang3@unl.edu)

D. Scott, Department of Biological Systems Engineering, Virginia Polytechnic Institute and State University, 312 Seitz Hall, Blacksburg, VA 24061, USA. (dscott@vt.edu)